Title

Operational Response of a Soil-Borehole Thermal Energy Storage System

Journal

Journal of Geotechnical and Geoenvironmental Engineering, 142(4)

ISSN

1090-0241

Authors

Başer, Tuğçe
Lu, Ning
McCartney, John S

Publication Date

2016-04-01

DOI

10.1061/(asce)gt.1943-5606.0001432

Peer reviewed

OPERATIONAL RESPONSE OF A SOIL-BOREHOLE THERMAL ENERGY STORAGE SYSTEM

Tuğçe Başer, M.S.[1], Ning Lu, Ph.D.[2] and John S. McCartney, Ph.D., P.E.[3]

ABSTRACT: This study focuses on an evaluation of the subsurface ground temperature distribution during operation of a Soil-Borehole Thermal Energy Storage (SBTES) system. The system consists of an array of five 9 m-deep geothermal heat exchangers, configured as a central heat exchanger surrounded by four other heat exchangers at a radial spacing of 2.5 m. In addition to monitoring the temperature of the fluid entering and exiting each heat exchanger, 5 thermistor strings were embedded in boreholes inside and outside of the array to monitor changes in ground temperature with depth. After 75 days of heat injection at a constant rate of 20 W/m, corresponding to 11.5 GJ of thermal energy, the average ground temperature in the array increased by 7 °C. However, depending on the storage volume definition, only 2.43 to 4.86 GJ of thermal energy was stored due to heat losses. After a 4-month rest period the heat storage was observed to decrease by 60% due to further heat losses. The trends in subsurface temperatures during heat injection were consistent with results from a simplified heat injection simulation using the system thermal conductivity estimated from a line source analysis. Although the heat injection rate of 20 W/m is smaller than that expected in actual SBTES systems (35-50 W/m), an energy balance analysis indicates the number of boreholes in the array was too few to effectively concentrate the heat injected within the subsurface. Nonetheless, the results provide an experimental reference point between a single borehole and a larger SBTES system.

[1] Graduate Research Assistant, University of California San Diego, Department of Structural Engineering, 9500 Gilman Dr. La Jolla, CA 92093-0085, USA. tbaser@ucsd.edu.
[2] Professor, Colorado School of Mines, Department of Civil and Environmental Engineering, 1500 Illinois St. Golden, Colorado, 80401, USA. ninglu@mines.edu.
[3] Associate Professor, University of California San Diego, Department of Structural Engineering, 9500 Gilman Dr. La Jolla, CA 92093-0085, USA. mccartney@ucsd.edu.

1. INTRODUCTION

Soil-Borehole Thermal Energy Storage (SBTES) systems are used to store heat collected from renewable sources so that it can be used later for heating of buildings (Claesson and Hellström 1981; Sibbitt et al. 2007; Chapuis and Bernier 2009; Sibbitt et al. 2012; Zhang et al. 2012; McCartney et al. 2013; Başer and McCartney 2015). They function in a similar way to conventional ground-source heat exchange (GSHE) systems, where heat is transferred from a source to a sink via circulation of fluid through a series of closed-loop heat exchangers. Because SBTES systems are meant to store heat, as opposed to exchanging heat without disturbing the ambient ground temperature, the spacing of the heat exchangers in SBTES systems is closer than that in conventional GSHE systems (Başer and McCartney 2015). They also differ from GSHE systems in that heat is primarily injected from renewable sources such as solar thermal panels during the summer months, and extracted for building heating during the winter months. During operation of SBTES systems using solar thermal panels as the heat source, the temperature of the ground within the array is expected to increase from its ambient temperature (approximately 10-20 °C) to potentially more than 60 °C (Sibbitt et al. 2012; Bjoern 2013), which is much higher than that encountered in conventional GSHE systems. One advantage of storing heat in the subsurface at temperatures around 60 °C is that heat can be transferred to and from the subsurface via direct circulation of fluid through the closed-loop heat exchangers without the aid of a heat pump. However, because Sibbit et al. (2007) noted that heat losses from SBTES systems can be 60% or more due to the high thermal gradients, Chapuis and Bernier (2009) proposed that the SBTES system store heat at lower temperatures to minimize the thermal gradient but incorporate a heat pump to help extract the heat from the circulating fluid. An additional difference between SBTES and GSHE systems is that the borehole heat exchanger

array in a SBTES system is overlain by a hydraulic barrier to retain pore water within the subsurface and an insulation layer to minimize heat losses to the atmosphere.

While SBTES systems are gaining popularity throughout the world, a better understanding of their thermal performance is required as their thermal storage capacity and heat loss highly depend on the average soil temperature during a heating or cooling period. Heat injection at temperatures around 30-60 °C may lead to different mechanisms of heat transfer for some soils than those expected under lower temperatures, with the potential onset of convective heat transfer in addition to conductive heat transfer (Lu 2001). The heat storage capacity of an SBTES system depends on the thermal properties of the subsurface and the different modes of heat transfer. Heat loss will occur from any SBTES system (upward, downward and laterally), and is dependent on the spacing of boreholes, number of boreholes, heat injection rate, and heat injection duration, along with the subsurface thermal properties (Başer and McCartney 2015). The primary mode of heat loss from an SBTES system is laterally to the surrounding subsurface. The upward and downward heat losses are not as significant because the area of heated soil around each borehole heat exchanger makes the vertical heat flux values much smaller than the lateral heat flux. Further, the upper surface of an SBTES system is typically insulated. The relative importance of heat losses decreases markedly as the size of the system increases, while it increases with the temperature difference between the storage and undisturbed ground temperature (Nordell and Hellström 2000). This paper investigates a relatively small array of boreholes forming a SBTES system, including a central borehole heat exchanger surrounded by four borehole heat exchangers at the same radial spacing. This provides an important reference point on the scalability of SBTES systems from a single borehole heat exchanger to a larger borehole array such at that at the DLSC site.

The operational concept of an SBTES system is shown in Figure 1. Heat is injected at a relatively constant rate during the summer months. During this time, the soil within the array increases in temperature. Heat is injected into the central borehole heat exchanger first, then to the surrounding borehole heat exchangers. Although the heat supply in most SBTES systems is from solar thermal panels that only produce heat for a certain period of time during the day, the heat injection rate is stabilized through the use of an intermediary fluid-filled heat storage tank (Sibbitt et al. 2007). The temperature of the soil increases rapidly due to the high thermal gradient, and the rate of increase in temperature decreases as the soil reaches its storage capacity. During the fall months, heat may continue to be injected into the array depending on the climate setting, or the heat injection may be stopped at the end of the summer. If heat injection is stopped, a rest period may occur, as shown in Figure 1, during which heat may be lost to the surrounding subsurface. After heat extraction in the winter, the system may recover some small amount of heat from the surrounding subsurface before heat is injected again into the array during the next summer.

Design parameters of SBTES systems include energy injection and extraction rates, borehole spacing as well as thermal properties of the subsurface. Two commonly used design models available for predicting the heat storage in SBTES arrays for variable injection and extraction rates are the duct storage (DST) model developed by Claesson and Hellström (1981) and Hellström (1989) and the superposition borehole model (SBM) developed by Eskilson (1987). As the borehole array investigated in this study was constructed for research purposes, it was not designed using these models to reach a certain energy storage needed for a building. Claesson and Hellström (1981) also proposed several analytical formulae based on the DST model for selecting the spacing of the boreholes, and found that the optimal spacing between borehole heat

exchangers in an SBTES system is 1.5-4.0 m. Başer and McCartney (2015) performed a series of simplified numerical analyses of heat conduction that indicate that soils with lower thermal conductivity have less lateral heat loss, and that arrays with smaller borehole spacing permit more concentrated storage of heat at higher temperatures.

The main objective of this study is to evaluate the temperature distribution in the subsurface during a heat injection test on a full-scale SBTES system installed in the vadose zone. Although the modes of heat transfer in the vadose zone are expected to be complex, this study does not focus on an evaluation of the potential coupled heat transfer and water flow within the array. Instead, it focuses on the effectiveness of a relatively small SBTES system in storing heat during a 4-month rest period after a 75-day heat injection period. Although there have been studies on the system thermal properties of the subsurface defined from short-term heat injection tests on single boreholes (Beier and Smith 2002; Gehlin and Spitler 2002; Lamarche et al. 2010; Raymond et al. 2011), the temperature distributions observed during long-term heat injection into multiple boreholes in this study provide an opportunity to evaluate transient interactions between heat exchangers in SBTES systems.

2. BACKGROUND

2.1. SBTES Systems

Although there have been several successful SBTES systems in Scandinavia since the late 1970's (Claesson and Hellström 1981), there are two recent examples of successful community-scale SBTES systems. The Drake Landing Solar Community (DLSC) in Alberta, Canada includes an SBTES system that has been in operation since 2007. This system supplies heat from solar thermal panels to an array of 144 borehole heat exchangers that are 35 m-deep and equally spaced at 2.25 m within a 35 m-wide grid. The SBTES system at this site has provided more than

90% of the heating requirements to 52 houses (Sibbit et al. 2012). The heat is transferred via direct of fluid through the borehole heat exchangers. Zhang et al. (2012) performed a numerical simulation of the heat exchange processes at the DLSC site, and found that the efficiency of heat transfer defined as the amount of heat extracted divided by the amount of heat injected is approximately 27%. Although this amount seems low, the thermal energy injected into the SBTES system is obtained freely from a renewable source and the heat extracted was sufficient to meet the needs of the community. Another successful SBTES system is in Braedstrup, Denmark, which also supplies heat from 18,000 m^2 of solar thermal panels to an array of 50 boreholes with a depth of 47-50 m and 3 m apart from each other installed across an area with a width of 15 m (Bjoern 2013). This system provides 14000 homes with 20% of their heat. At both sites, heat is permitted to escape laterally from the SBTES array. The DLSC site includes a hydraulic barrier to minimize evaporation of water from the soil (the groundwater table is 6 m below the ground surface).

2.2. Heat Injection Tests

Heat transfer in the subsurface has primarily been studied as a time-dependent heat conduction problem due to the complexities involved when considering convection. Heat transfer from a borehole heat exchanger to the subsurface depends on the thermal conductivity of the ground as well as the heat injection rate and the undisturbed ground temperature. Thus, a proper design of a ground source energy system requires a good estimation of the ground thermal properties. The thermal response test (TRT) is routinely used to determine the ground thermal properties as well as the heat-transfer performance between the ground and the heat exchanger (Mogensen 1983; Gehlin and Spitler 2002). In a TRT, heat is injected into a vertical geothermal heat exchanger within a borehole at a constant rate. Specifically, heated fluid is pumped through

the heat exchanger tubing and the inlet and outlet fluid temperatures are measured as a function of time, along with the power input to the heater and the fluid flow rate (Gehlin and Spitler 2002). The heat injection rate can be calculated from these variables as follows (Carslaw and Jaeger 1959):

$$\dot{Q} = \dot{V}_f \rho_f C_f \left(T_{in} - T_{out}\right) \quad (1)$$

where $\dot{V}_f$ is the volumetric flow rate of fluid (m^3/s), ρ_f is the fluid density (kg/m^3), C_f is the specific heat capacity of the fluid (J/(kgK)), and T_{in} and T_{out} are the temperatures of the fluid entering and exiting the heat exchanger loops, respectively (K).

During a TRT, the average of the inlet and outlet fluid temperatures is plotted as a function of time to evaluate the increase in the ground temperature as a function of time. This data can be interpreted using solutions to Fick's equation considering only heat flow via conduction, such as the infinite line source, finite line source, and cylinder source (Mogensen 1983; Eskilson 1987; Witte et al. 2002; Gehlin and Spitler 2002). The infinite line source equation is the simplest solution, where the thermal conductivity λ of the soil surrounding an infinite source during application of a constant heat injection rate $\dot{Q}$ can be calculated as follows:

$$\lambda = \frac{\dot{Q}}{4\pi L}\left[\frac{dT}{d\left(\ln t\right)}\right]^{-1} \quad (2)$$

where L is the length of borehole heat exchanger. The term in brackets is the slope of the change in mean fluid temperature versus the logarithm of time. This slope is typically calculated after the slope of the temperature rise curve has stabilized, which typically corresponds with the time that the heat capacity of the heat exchanger and grout is reached. The line source analysis and the others mentioned above assume that the subsurface is homogeneous, and provide a system value of thermal conductivity for the subsurface even if there are multiple strata with different thermal

properties. Recently, it has been proposed to also measure temperature variations along the boreholes to determine the thermal properties as a function of depth using the Distributed Thermal Response Test (DTRT) (Acuna and Palm 2013). Another alternative is to use embedded instrumentation in the ground around a heat exchanger to measure the temperature gradient and infer the subsurface thermal properties by assuming the mode of heat transfer (Murphy et al. 2014).

3. FIELD TEST

3.1. Overview

The heat injection test described here was performed on a SBTES system on the Colorado School of Mines campus in Golden, CO (US) between June-September 2014. The SBTES system under investigation consists of an array of five 9 m-deep geothermal heat exchangers installed in vertical boreholes having a diameter of 70 mm (BH-1 to BH-5), configured as a central heat exchanger surrounded by four others at a radial spacing of 2.5 m, as shown in Figure 2(a). The array is overlain by a hydraulic barrier, an insulation layer, and a layer of site soil to support vegetation, as shown in Figure 2(b). Thermistor strings were installed in the same holes as the heat exchangers in BH1 and BH2 to observe the temperature changes at the locations of the heat exchangers during the heating and cooling periods (T-A and T-C). Three additional boreholes were drilled at locations inside and outside of the array for installation of thermistor strings to observe changes in ground temperature (T-B, T-D, and T-E).

The heat exchange tubing consisted of 25.4 mm-inner diameter cross-linked polyethylene (PEX) tubing having a thermal conductivity of 0.4 W/(m°C), configured in a “U” shape. After placement of the heat exchange tubing or the thermistor string, sand-bentonite grout with a mixture ratio of 4:1 sand to bentonite was backfilled into the space between the U-loop tube and

the inner BHE wall. The grout has a thermal conductivity of 1.20 W/(m°C). The top of the system included a 60 mil (1.52 mm)-thick high-density polyethylene geomembrane hydraulic barrier to minimize evaporation from the subsurface, and a 60 mm-thick expanded polystyrene insulation layer to minimize upward heat loss. Before placing the hydraulic barrier and insulation layer, the heat exchanger tubing coming out of the boreholes was wrapped with foam insulation then routed below the surface through a 1-m deep trench to the location of the manifold.

3.2. Subsurface Conditions

The subsurface conditions were assessed during drilling of the first borehole, which was drilled using an air hammer bit. The majority of the subsurface consists of a colluvial deposit of dry, cemented sandy gravel, extending to a depth of 7 m below the surface. Below this a 1 m-thick sand layer was encountered, which was underlain by stiff clay. The water table coincided with the top of the sand layer at a depth of 7 m from the surface. The remaining boreholes were drilled using the slurry method due to the saturated sand layer. The thicknesses of the soil layers observed during drilling of the first borehole are presented in Figure 2(b).

3.3. Instrumentation

Temperature variations in the soil inside and outside of the SBTES system were monitored using five thermistor strings (T-A to T-D) from Geokon Inc. of Lebanon, NH. The thermistor strings consist of a single cable with four thermistors located at different lengths. The thermistor strings were inserted into the boreholes shown in Figure 2(a), after which the boreholes were backfilled with sand-bentonite grout. They were either attached to a metal stinger to hold them in place during grout placement, or were attached to the heat exchanger tubing with tape. One of the thermistor strings was installed in a borehole outside of the insulated array to provide a measure of the surrounding subsurface temperature. Each thermistor string was connected to a

MICRO-1000 Data logger that has a 32 channel multiplexer. In addition to the thermistor strings, thermistor pipe plugs (Model TC-J-NPT-G-72 from Omega, Inc.) were used to measure the temperature of the fluid entering and exiting each borehole heat exchanger, as shown in Figure 2(b). The manifold shown in Figure 2(b) was insulated, but was not in an enclosed building, so the temperatures measured using the thermistor pipe plugs are slightly affected by daily fluctuations in air temperature. However, the temperature of the heated fluid is much greater than these fluctuations so it did not play a major role in interpretation of the results.

3.4. Field Testing Procedures

A Geocube^{TM} heating device from Precision Geothermal of Maple Plain, MN was used to inject heat into the SBTES array by heating and circulating a 20% mixture by weight of propylene glycol and water for a total of 75 days during the summer of 2014. The mixture has a density of 1008 kg/m^3 and a specific heat capacity of 3267 J/(kg°C). The heating device has a maximum heating capacity of 11 kW through the use of four heating elements in series (2×2500 W and 2×3000 W). However, only a single heating element having a capacity of 2500 W was used in this study to avoid high fluid temperatures that would have triggered the overheating sensor in the heating device. The SBTES system in this study has a relatively short heat exchanger length of approximately 100 m (including both legs of the U-tubes) compared to some GSHE systems that can be tested using the heating device. The fluid was first injected into the central borehole (BH-1) at an average flow rate of 500 ml/s, after which the return fluid was split into the other four boreholes at different flow rates, then back into the heating device, as shown in Figure 2(b). The sequence of the flow paths are numbered in the Figure 2(b), showing that flow first goes into the central borehole (1), comes out of the central borehole (2), is split at the location of the manifold into the four surrounding boreholes (3), comes out of the four boreholes

(4), then is sent back to the heater (5). The flow rate through each of the five boreholes was controlled using a special ball valve (Model 58A from Apollo, NC) that has a Venturi orifice. The pressure drop across the Venturi orifice can be measured to estimate the flow rate through the valve. A differential pressure gage from Differential Pressure Plus, Inc. (Model 200 DPG) was used to measure the water pressures on either side of the Venturi orifice during testing. Although the ball valves were adjusted with the goal of equally distributing the flow through the four outer boreholes, the fluid temperatures, which will be discussed later, indicate that the flow rate through BH-2 may not have been equal to the others. During the heat injection period, the inlet and outlet temperatures of the heat exchanger fluid for each borehole were continuously monitored using pipe plug thermistors installed within the ball valves on the manifold. After the 75 days of heat injection, the ground was left to rest so that the ambient heat loss could be characterized over a period of 4 months. During this time, the ground temperature was monitored using the thermistor strings, and there was no fluid flow through the borehole heat exchangers.

4. RESULTS

4.1. Flow Rate and Temperatures of the Heat Exchanger Fluid during Heat Injection

The actual flow rate supplied as a function of time to the central borehole (BH-1) measured using the heating device is shown in Figure 3(a). A decrease in flow rate was observed over time, potentially due to a reduction in efficiency of the circulating pump as the temperature of the fluid increased. An issue that occurred during the test is that the manifold was rotated 90 degrees while the test was running due to construction at the site not associated with the experiment. This can be observed as a sudden reduction in the flow measurement data after 49 days of operation.

247 The average fluid flow rates before and after the manifold was rotated are summarized in
248 Table 1.

249 As mentioned, the differential pressure gage was inserted into the P-T ports to infer the flow
250 rates through the four outer borehole heat exchangers, and the balancing values were adjusted in
251 an attempt to split the flow exiting from BH-1 evenly between the others. However, the
252 balancing was not perfect and BH-2 ended up receiving less flow than BH-3, BH-4, and BH-5.
253 This was not assessed until the end of the test when physical flow measurements were made for
254 each of the borehole heat exchangers. It is possible that after the manifold orientation was
255 changed that the distribution in flow rate through the four outer boreholes could also have
256 changed, but it is not possible to estimate this quantitatively. Accordingly, the flow rates for BH-
257 2 to BH-5 were assumed to be fractions of BH-1 estimated from the physical flow measurements
258 at the end of the test, as shown in Figure 3(a). Despite the unbalanced flow, the flow rates in the
259 boreholes shown in Figure 3(a) are sufficient to reach turbulent flow conditions (or at least
260 transitional conditions for BH-2), which maximizes convective heat transfer from the circulating
261 fluid into the ground.

262 The temperature of the heat exchange fluid entering and exiting each borehole heat
263 exchanger may be different due to differences in the flow rate and local variations in the heat
264 transfer into the ground. The heat exchanger fluid temperatures as a function of time are shown
265 in Figures 3(b) to 3(e) for the five heat exchangers. The difference in the inlet and outlet
266 temperatures, $\Delta T_{in\text{-}out}$, is also shown in these figures, which together with the flow rate in Figure
267 3(a) reflects the magnitude of heat exchange following Eq. 1. The positive sign of $\Delta T_{in\text{-}out}$
268 confirms that the SBTES system is in heating mode. The highest temperature difference was
269 recorded at BH-2 and the lowest was observed in the center borehole (BH-1). The low

temperature difference in BH-1 may be due to the greater flow rate through this heat exchanger that may not have permitted as much residence time for heat transfer into the ground as in the other heat exchangers. Another issue is that the temperature differences started to rise slowly for all of the borehole heat exchangers because of decreasing flow rates after the manifold configuration was changed. Although the trends in the temperature difference changed throughout the test, the average fluid temperatures can be used to characterize the boundary conditions for each borehole heat exchanger throughout the test.

For a given flow rate, a higher value of $\Delta T_{in\text{-}out}$ represents a higher amount of heat injected into the ground. The value of $\Delta T_{in\text{-}out}$ ranged from 0.2 to 5.3 °C with an average of 1.8 °C. The heat injection rates per unit length (using both the downward and upward lengths of tubing) calculated using Eq. 1 are summarized in Table 1. The average heat injection rate per unit length for all of the boreholes is 20 W/m. Although the heat exchange capacity of a GSHE system depends on the thermal properties of the different materials and geologic strata, groundwater flow, borehole dimensions, heat exchanger configuration, in deep geothermal systems (i.e., 200 m), the difference between inlet and outlet fluids is typically 2 °C in most systems (Schiavi 2009). This may be higher in SBTES systems, which have a heat injection rate of 35 W/m or greater (Acuna and Palm 2013).

4.2. Surface Air and Ground Temperatures

The maximum, minimum, and average temperatures of the air in Golden, CO during the duration of the heat injection and rest periods are shown in Figure 4(a) for reference. Although there SBTES array is 1 m below the ground surface along with an insulation layer, the air temperature still may have an effect on the subsurface temperatures around the array. The

292 temperature is observed to range from almost 35 °C in the summer to -25 °C in the winter, with a
293 significant temperature drop in November 2014.

294 Time series of the ground temperatures during the test are shown in Figures 4(b) to 4(e).
295 Before the heat injection test, the ground temperatures were monitored for a period of one month
296 to help ensure that the thermistors were in equilibrium with the ambient ground temperature.
297 Despite the insulation layer at the surface of the SBTES, the temperature at different depths in
298 the array still varied between 9 and 13 ºC because of the previous seasonal effects on the ground
299 temperature, with greater temperatures near the ground surface due to the spring heating. This
300 temperature range is reflected in the initial temperatures shown in the figures for the different
301 depths.

302 Heat injection led to an increase in ground temperatures measured by the thermistor strings.
303 The horizontal dotted lines in Figure 4 denote the "average initial temperature" with depth in
304 each borehole that was given as a reference line to compare the temperatures with the initial
305 conditions. It should be noted that the background temperature may fluctuate seasonally up to a
306 certain depth (approximately 2 m), which can change the amount of heat storage compared to the
307 ambient ground temperature. The vertical dashed lines denote the end of the heat injection phase.
308 The ground temperature reached a maximum temperature of 32.5 °C at a depth of 9 m at the
309 central borehole BH-1, as shown in Figure 4(a). The temperature at the surrounding borehole
310 heat exchangers increased up to a lesser amount (25 °C) as shown in Figure 4(d) for BH-2. The
311 soil within the array also experienced an increase in temperature, which was between that of
312 BH-1 and BH-2, as shown in Figure 4(c). Further, a clear delay in temperature rise was observed
313 at this location compared to the locations of the borehole heat exchangers. Although T-D was
314 located outside of the array, and was not covered by the insulation layer, it was still affected by

315 the heat injection process, as shown in Figure 4(e). It should be noted that during heat extraction
316 from the SBTES, the borehole heat exchangers might be able to extract heat from the subsurface
317 outside of the array as well. This is one reason that Başer and McCartney (2015) defined the
318 storage volume of the array as 2 radial spacings from the center. Comparing T-D and T-E, which
319 is at the outside edge of the array, the role of the insulation layer and overlap in heating from
320 BH-1 and BH-2 is reflected in the slightly higher temperatures at the location of T-E, as shown
321 in Figure 4(f). Although one of the sensors in thermistor string T-B at depth of 6 m ceased
322 operating after 49 days of operation, there was good survivability of the thermistors in the
323 system.

324 After 75 days of heat injection, the ground was permitted to rest to observe ambient heat loss
325 from the system. Overall, the highest temperature change was observed at a depth of 2.3 m near
326 the ground surface, while the lowest was observed at 9 m. Despite the surface insulation layer
327 (located 1.3 m above the uppermost thermistors), the data from these thermistors indicates that
328 heat loss will still occur upwards due to the very cold air temperatures observed in Figure 3(a).
329 The ground temperature at the locations of the borehole heat exchangers decreased drastically at
330 the start of cooling but stabilized after 60 days in almost all thermistor locations. The same
331 behavior was observed in the temperature distribution from the thermistors installed between
332 heat exchangers, which reflects spreading of the heat throughout the array. Outside of the array,
333 the ground was still on average at least 2.5 °C greater than at the beginning of the heat injection
334 period. Although this increase in temperature is not significant, it still reflects a substantial
335 amount of thermal energy (0.65 GJ) across the volume of the array. A heat pump would likely be
336 necessary to extract this heat efficiently for this small size of array. The SBTES system at DLSC
337 is different, as the large number of boreholes in the array permits the ground to increase in

temperature by almost 50 °C above the ambient ground temperature, so only direct circulation is needed to extract the heat.

Temperature profiles with depth at different times after the start of heating are shown in Figure 5. Due to the contact between heat exchangers and sensors, the temperatures are more uniform with depth in T-A and T-C. However, the highest temperature increase was observed in the center borehole. The soil throughout the height of the soil layer was observed to increase in temperature steadily over time during heat injection. The highest increases in temperatures were observed near the top of the array. This could be due to the effect of the insulation layer near the surface, but it could also reflect upward vapor flow in the soil layer due to phase change. As the pore water in the soil heats up, it may vaporize and move upwards due to buoyancy, carrying heat through convection. This is a mode of heat transfer in SBTES systems that will be investigated in future studies using advanced numerical simulations.

The temperature of the ambient ground outside of the array was not measured, but was predicted using the analytical model presented by Brandl (2006), given as follows:

$$T(z,t) = T_{m,out} + \frac{\Delta T_{out} e^{-z/d}}{\sqrt{1+2k+2k^2}} \cos\left(\omega(t-\varepsilon) - \frac{z}{d}\right) \quad (3)$$

where z is the depth from the surface, t is the time, $T_{m,out}$ is the mean yearly air temperature, ΔT_{out} is the amplitude of outside air temperature, ω is the frequency of temperature fluctuations, d is the damping depth of temperature fluctuations, and k is a heat transfer coefficient that depends on the soil-atmosphere interaction coefficient a_s. The parameters of the model are presented in Figure 5(f). The temperature parameters were selected so that the calculated value at the surface T(0,t) matched the air temperature fluctuations shown in Figure 4(a). The predictions shown in Figure 5(f) are consistent with the initial temperatures in the site, and indicate that the temperature should not fluctuate significantly seasonally below a depth of d = 1.65 m.

Temperatures from thermistor strings T-B through T-D are plotted versus radial distance from the center borehole for 4 different depths are shown in Figure 6. As observed from the evaluation of the time series in Figure 4, the greatest temperature was observed at the center of the array, with a slightly lower temperature at the location of BH-2. The highest increase in temperature was observed at the depth of 2.3 m inside of the array. The increase in temperature is greater at T-B than at T-D, as T-B is in between two heat exchangers. As the test proceeds, while temperatures in the array increase, temperatures outside of the array remain almost constant except closer to the surface. The increase in temperature inside the array ranged from 4 to 6 °C at different depths, while it was 1 ºC outside of the array at the end of heating. This corresponds to a temperature ratio of about 5 comparing the temperature within the array to the temperature outside of the array. At the end of heat injection, a rapid decrease was observed in T-A and T-C because of the contact between the strings and the heat exchangers. However, the temperature within the array started to become more uniform with radial location from the center.

5. ANALYSIS

5.1. Evaluation of Subsurface Thermal Properties

Although it is not the primary goal of this paper, the fluid and ground temperature results presented in the previous section permit an assessment of the subsurface thermal properties. First, the mean fluid temperatures of the boreholes versus time were plotted in a semi-logarithmic scale were assessed to calculate the system thermal conductivity using the line source analysis, using Eq. 2. The system thermal conductivity ranged from 0.52 to 0.57 W/(m°C), which is relatively low but is consistent with the thermal conductivity dry, sandy gravel conglomerate. As the heating test is longer than a conventional thermal response test,

thermal conductivity was calculated for three different time intervals as shown in Table 1, at early times typical of most thermal response tests, at a middle-range of time, and late in the heat injection test after rotation of manifold caused the change in flow rate. At the later times of heat injection, it is possible that interaction between the boreholes starts to violate the assumptions of the line source analysis and affect the thermal properties calculated using this approach. Despite some minor variations, the thermal conductivity of the subsurface was similar and consistent for each of the heat exchangers, and an average value of 0.54 W/(m°C) was assumed to be representative of the system. Although low, Başer and McCartney (2015) found that lower thermal conductivities are desirable for SBTES systems to minimize heat losses from the system.

Although the ground temperature data shown in Figure 6 may be used to estimate the thermal gradients to infer the subsurface thermal properties by assuming the mode of heat transfer to be conduction (Murphy et al. 2014), there are two issues that prevented this analysis from being performed in this study. The first is that the temperatures at the monitoring boreholes are affected by multiple heat exchanger arrays. Second, the temperature distribution away from the heat exchanger is expected to be highly nonlinear leading to inaccuracies in the gradient calculated between two observation points within the array. This indicates that numerical simulations are more suited for further evaluation of heat transfer processes within SBTES systems.

5.2. Comparisons with Numerical Simulations

In order to check the magnitudes and trends in ground temperature measured in the field test, a three-dimensional, transient finite element model developed in COMSOL Multiphysics (Version 4.4b) was used to predict the temperature distribution within the borehole array. Although it is possible that phase change and convection occurred in the unsaturated conglomerate layer, performing a conductive-convective heat transfer analysis requires several

406 input parameters outside the scope of this study. Accordingly, heat transfer in the simulation was
407 assumed to be by conduction alone for simplicity. The model considers the geometry of the
408 SBTES system in Figure 2 consisting of five boreholes (one at the center) with a depth of 9 m
409 and with an equal borehole spacing of 2.5 m. The thermal conductivity from line source analysis
410 (λ = 0.54 W/(m°C)) was used in the simulation, along with the other thermal properties listed in
411 Table 2. The specific heat of the conglomerate was inferred from SH-1 thermal needle probe
412 measurements at the ground surface, although variations were observed due to the
413 nonhomogeneous material. The density of the conglomerate near the surface was estimated using
414 the sand cone test. The thermal properties of the lower layers were assumed based on reasonable
415 ranges for these materials, but they were not found to have a major impact on the results of the
416 analysis.
417 An example of the simulation mesh used in this study was presented in Başer and McCartney
418 (2015). The boundary heat flux applied on the borehole walls as well as the thermally insulated
419 layer at the top of the soil layer that represents the insulation layer in the field. The initial
420 temperature of the system was assumed to be uniform with depth and equal to the average initial
421 reading of the thermistor strings (12 °C). The temperature distributions at a depth of 7.8 m at the
422 end of 75 days of heating are shown in Figure 7. Although the magnitude of the numerical
423 simulations did not match well with the experimental results in all locations, the trends in the
424 temperature with radial location match those in the experiment. The numerical simulation also
425 reveals the large gradients in temperature that can occur around the borehole heat exchangers,
426 which could not be assessed from the thermistor string data.
427

5.3. Heat Storage Analysis

The success of a SBTES system depends on the heat stored within the borehole array during the resting period after heat injection stops. The thermal energy stored (J) is equal to the difference between the cumulative amounts of thermal energy injected into the subsurface and the amount of heat lost from the array, which can be expressed as follows:

$$Q_{stored} = Q_{injected} - Q_{lost} \quad (4)$$

An energy balance analysis using Equation 4 relies upon estimates of the total thermal energy injected into the subsurface as a function of time (i.e., using Equation 1), along with estimates of the heat loss out of the volume of the array (i.e., upward, downward, and laterally), which require experimental data and some estimate of the volume of the array. The heat loss from an SBTES system is expected to increase over time during heat injection due to the higher thermal gradient between the array and the free-field ground temperature. If it is possible for a SBTES system to reach its thermal storage capacity, the rate of lateral heat loss at this point is expected to approach the rate of heat injection. It is typically assumed that the heat transfer upward and downward are negligible compared to the lateral heat loss in this analysis, mainly due to the relatively small area of heat transfer compared to the lateral heat loss from the system as reflected in the temperature profiles from the COMSOL analysis in Figure 7. Further, the upward heat loss is also assumed to be negligible due to the insulation layer placed on top of the array. Accordingly, the lateral heat loss is assumed to be the primary mode of heat loss from the array.

As it may be difficult to estimate the heat losses from the array using the experimental data available in this study, the approach of Claesson and Hellström (1981) can be used to quantify the average total thermal energy storage as follows:

$$Q_{stored} = (T_s - T_a) C_v \pi r^2 H \quad (5)$$

where (T_s-T_a) is the temperature difference between storage and surrounding subsurface, C_v is the volumetric heat capacity of the soil (J/m^3K), r is the radius of a cylindrical storage volume (m), and H is the height of the storage volume (m). The challenge of using this approach is that the volumetric heat of the soil may change with time due to changes in the degree of saturation of the soil, and may also differ with depth and radial distance within the array. It is also challenging to define the volume of the array to use in the calculations. Two array volumes were considered in the analysis, 1 radial spacing from the center (2.5 m) where the average temperature within the array was taken as a transient average of the measurements from T-B and T-C, and 2 radial spacings from the center (5.0 m) where the average temperature within the array was taken as a transient average of the measurements from T-B, T-D, and T-E. The second spacing is consistent with Başer and McCartney (2015), who defined the storage volume as 1 radial spacing outside of the outermost boreholes (2 radial spacings from the center) because the heat outside of the outermost boreholes may be able to be recovered during heat extraction. The baseline temperature in both calculations was assumed to be the initial ground temperature, and the fluctuations in temperature near the surface observed in Figure 5(f) were not considered. The calculation of the average ground temperatures within the array using the results from T-B, T-D, and T-E is conservative, as it does not consider the high temperatures near the boreholes.

The energy balance of the system using this approach is shown in Figure 8. The heat stored as a function of time follows the trend in internal array temperatures observed in Figures 4(c) and 4(e). The heat loss during heat injection was observed to be higher than the heat storage, which can be explained by the high gradients. After heat injection stopped, the heat loss still increased, but at a decreasing rate. Approximately 2.43 to 4.86 GJ were available at the end of the heat injection period depending on the array volume assumed, and 0.65 to 1.32 GJ were available

after the end of the resting period. For reference, an energy efficient house with a floor area of 100 m^2 has a heat demand of 12 GJ/year (Reuss and Mueller 1999), so for this array to be effective, a greater heat injection rate over a longer period should have been used. Although the heat injection rate evaluated in this study is lower than that expected in actual SBTES systems, the amount of heat stored in the soil at the end of the heat injection period is not negligible, especially considering the fact that solar thermal panels provide an essentially free heat source.

The results from the energy balance calculations indicate that the SBTES array evaluated in this study was not able to effectively concentrate heat in the subsurface at the same temperatures encountered in the DLSC site (greater than 60 °C) and counter the effects of lateral heat loss. This observation could have due to the fact that the array did not have a sufficient enough number of boreholes. To evaluate this possibility, simple numerical analyses with conduction as the sole means of heat transfer were performed to assess the impact of the number of heat exchangers on the temperature distribution within an array. The results are shown in Figure 9 for a heat injection rate of 20 W/m for the times after heat injection and after a resting period. The fewer the number of heat exchangers, the greater the amount of heat lost from the array at the edges. Arrays with a greater number of boreholes will reach an average temperature that may be greater than the overlap in temperature between two boreholes, as lateral heat loss only occurs at the edges. The main implication of using an SBTES system with a smaller array is that a heat pump may be needed to extract a sufficient amount of heat to cover the heating demands of a structure. This is in contrast to a large-scale SBTES system such as that at DLSC, where direct circulation of fluid through the heated soil was sufficient to extract heat for heating of buildings (Sibbitt et al. 2012). It should be noted that Zhang et al. (2012) found that the efficiency of heat

494 extraction at DLCS is only 27% due to the heat loss of approximately 60%, even though the
495 system is still able to provide 90% of the heating demands of the community.

496 ## 6. CONCLUSIONS

497 This study focused on the temperature response of a soil-borehole thermal energy storage
498 (SBTES) system installed in the vadose zone in Golden, CO. The instrumentation at the site
499 permitted evaluation of the thermal properties of the subsurface as well as the heat storage
500 characteristics of the array as a function of time during a heat injection period and a rest period.
501 The system thermal conductivity estimated from a thermal response test on the group of
502 boreholes in the array was used in numerical simulations of conductive heat transfer to predict
503 the temperature distribution in the borehole array, and a good match was obtained. Although it is
504 possible that combined convective and conductive heat flux may have occurred in the SBTES
505 system in the vadose zone, further research is needed to quantify the different material properties
506 that can be used in advanced numerical simulations that capture all modes of heat transfer. A
507 heat balance analysis performed using the measured field data indicates that a substantial portion
508 of the injected heat left the array due to lateral heat loss, and that a greater heat injection rate
509 would be necessary to meet the thermal demands of a typical residence. The SBTES system
510 evaluated in this study is the next smallest array beyond a single borehole, and the thermal
511 response of this array permitted an evaluation of the scalability of this type of system. Arrays
512 with a greater number of boreholes were found to more effectively concentrate heat and
513 minimize the effects of lateral heat loss.

514 ## ACKNOWLEDGEMENTS

515 Funding from National Science Foundation (NSF 1230237) is much appreciated. The
516 opinions are those of the authors alone and do not reflect the viewpoint of the sponsor.

REFERENCES

Acuna, J. and Palm, B., 2013. Distributed thermal response tests on pipe-in-pipe borehole heat exchangers. Applied Energy. 109, 312-320.

Austin, W.A., 1998. Development of an In-situ System for Measuring Ground Thermal Properties. M.S. Thesis. Oklahoma State University, Stillwater, OK.

Başer, T. and McCartney, J.S. 2015. Development of a full-scale soil-borehole thermal energy storage system. Proceedings of the International Foundations Conference and Equipment Exposition (IFCEE 2015). San Antonio, TX. Mar. 17-21. ASCE. pp. 1-10.

Beier, R.A. and Smith, M.D., 2002. Borehole thermal resistance from line-source model of in-situ tests. ASHRAE Transactions. 108(2), 212-219.

Bjoern, H. 2013. Borehole thermal energy storage in combination with district heating. European Geothermal Congress 2013. Pisa. June 3-7. 1-13.

Carslaw, H.S. and Jaeger, J.C., 1959. Conduction of Heat in Solids. Oxford Clarendon Press, 2nd Edition. 517 p.

Chapuis, S. and Bernier, M., 2009. Seasonal storage of solar energy in borehole heat exchangers. Proc. of the IBPSA Conf. on Building Simulation. Glasgow. 599-606.

Claesson, J. and Hellström G., 1981. Model studies of duct storage systems. New Energy Conservation Technologies and their Commercialization. J.P. Millhone and E.H. Willis, Eds. Springer-Verlag, Berlin. 762-778.

Eskilson, P., 1987. Thermal Analysis of Heat Extraction Boreholes. Lund, Sweden: Dept. of Mathematical Physics, University of Lund.

Gehlin, S., 2002. Thermal response test- Method development and Evaluation. Doctoral Thesis. Lulea University of Technology, Lulea, Sweden.

Gehlin, S. and Spitler, J.D., 2002. Thermal Response Test - State of the Art. Report IEA ECES Annex 13.

Hellström, G., 1989. Duct Ground Heat Storage Model: Manual for Computer Code. Lund, Sweden: University of Lund.

Lamarche, L., Kajl, S., Beauchamp, B., 2010. A review of methods to evaluate borehole thermal resistances in geothermal heat-pump systems. Geothermics. 39(2), 187–200.

Lu, N. 2001. An analytical assessment on the impact of covers on the onset of air convection in mine wastes. International Journal of Numerical and Analytical Methods in Geomechanics, 25, 347-364.

McCartney, J.S., Ge, S., Reed, A., Lu, N., and Smits, K. 2013. Soil-borehole thermal energy storage systems for district heating. Proceedings of the European Geothermal Congress 2013. Pisa. Jun. 3-7. European Geothermal Energy Council, Bruxelles.1-10.

Mogensen, P., 1983. Fluid to duct wall heat transfer in duct system heat storages. Proc. Int. Conf. on Subsurface Heat Storage in Theory and Practice. Stockholm. June 6-8, 652-657.

Murphy, K.D., Henry, K.S., and McCartney, J.S. 2014. Impact of horizontal run-out length on the thermal response of full-scale energy foundations. Proceedings of GeoCongress 2014 (GSP 234), M. Abu-Farsakh and L. Hoyos, eds. ASCE. pp. 2715-2714.

Nordell, B. and Hellström, G., 2000. High temperature solar heated seasonal storage system for low temperature heating of buildings. Solar Energy. 69(6), 511–523.

Raymond, J., Therrien, R., and Gosselin, L., 2011. Borehole temperature evolution during thermal response tests. Geothermics. 40(1), 69-78.

Reuss, M. and Mueller, J.P., 1999. Solar district heating with a combined pit and duct storage in the underground. ISES Solar World Congress. Vol. 3, 468-483.

563 Schiavi, L., 2009. 3D simulation of the thermal response test in a U-tube borehole heat
564 exchanger. Proc. of COMSOL Conference. Milan. Oct. 14-16. 1-7.
565 Sibbitt, B., Onno, T., McClenahan, D., Thornton, J., Brunger, J., and Wong, B., 2007. The Drake
566 Landing solar community project – early results. Canadian Solar Buildings Conference.
567 Calgary, June 10-14. 1-8. (CD-ROM).
568 Sibbitt, B., McClenahan, D., Djebbara, R., Thornton, J., Wong, B., Carriere, J., and Kokko, J.,
569 2012. The performance of a high solar fraction seasonal storage district heating system –
570 Five years of operation. Energy Procedia, 30, 856-865.
571 Smits, K.M., Sakaki, S.T., Howington, S.E., Peters, J.F., and Illangasekare, T.H. 2013.
572 Temperature dependence of thermal properties of sands across a wide range of
573 temperatures (30-70 °C). Vadose Zone Journal, doi: 10.2136/vzj2012.0033.
574 Witte, H.J.L., van Gelder, G.J., and Spitler, J.D., 2002. In situ measurements of ground thermal
575 conductivity: The Dutch perspective. ASHRAE Transactions, 108(1), 263–72.1.
576 Zhang, R., Lu, N., and Wu, Y., 2012. Efficiency of a community-scale borehole thermal energy
577 storage technique for solar thermal energy. GeoCongress 2012. ASCE. 4386-4395.

TABLE AND FIGURE CAPTIONS

Table 1. Fluid flow rates, average heat injection rates and system thermal conductivity estimates from the line source analysis

Table 2. Thermal properties for the different soil layers used in the numerical simulations

Figure 1. Typical operational periods for an SBTES system along with ground temperature trends at the center of the array

Figure 2. Schematics of the SBTES system (not to scale): (a) Plan view; (b) Elevation view

Figure 3. Temperature boundary conditions during the heat injection test: (a) Flow rates for each BH; (b) Inlet and outlet temperatures of the fluid circulating within the heat exchange loops in borehole BH-1; (c) BH-2; (d) BH-3; (e) BH-4; (f) BH-5

Figure 4. Temperature time series: (a) Surface air; (b) T-A; (c) T-B; (d) T-C; (e) T-D; (f) T-E

Figure 5. Temperature profiles from thermistors: (a) T-A; (b) T-B; (c) T-C; (d) T-D; (e) T-E; (f) Predicted seasonal ground temperature fluctuations

Figure 6. Temperature profiles with radius for different depths from surface: (a) 2.3 m; (b) 6.0 m; (c) 7.8 m; (d) 9.0 m

Figure 7. Comparison between radial distributions in ground temperatures measured in the experiment and predicted using the numerical analysis of conductive heat transfer

Figure 8. Evaluation of the thermal energy balance in the SBTES during the heat injection and resting phases

Figure 9. Examples of heat storage in SBTES systems of different scales after heat injection at a rate of 20 W/m for 90 days and after the end of a 90 day rest period

599 Table 1. Fluid flow rates, average heat injection rates and system thermal conductivity estimates

600 from the line source analysis at different times

Borehole	Average flow rate (0 to 49 days) (ml/s)	Average flow rate (49 to 75 days)* (ml/s)	Average heat injection rate (W/m)	Thermal conductivity (1-4 days) (W/(m°C))	Thermal conductivity (12-17 days) (W/(m°C))	Thermal conductivity (49-75 days) (W/(m°C))
1	500	300	18.6	0.48	0.52	0.55
2	50	30	18.5	0.45	0.55	0.54
3	150	83	23.1	0.56	0.54	0.66
4	150	83	19.4	0.55	0.57	0.55
5	150	83	19.3	0.54	0.57	0.55

601 *After rotation of manifold

602

603 Table 2. Thermal properties for the different soil layers used in the numerical simulations

Layer	Depth to layer interface from surface (m)	Thermal conductivity (W/(m°C))	Specific heat capacity (J/(kg°C))	Total density (kg/m^3)
Expanded polystyrene insulation	0.8	0.03	900	1005
Colluvial deposit (cemented sandy gravel)	1.0	0.54	1200	1650
Alluvial sand deposit	7.0	1.80*	1200*	1650*
Stiff clay deposit	8.0	1.00*	1400*	1700*

604 *Estimated values

Figure 1
Click here to download Figure: Fig 1.tif

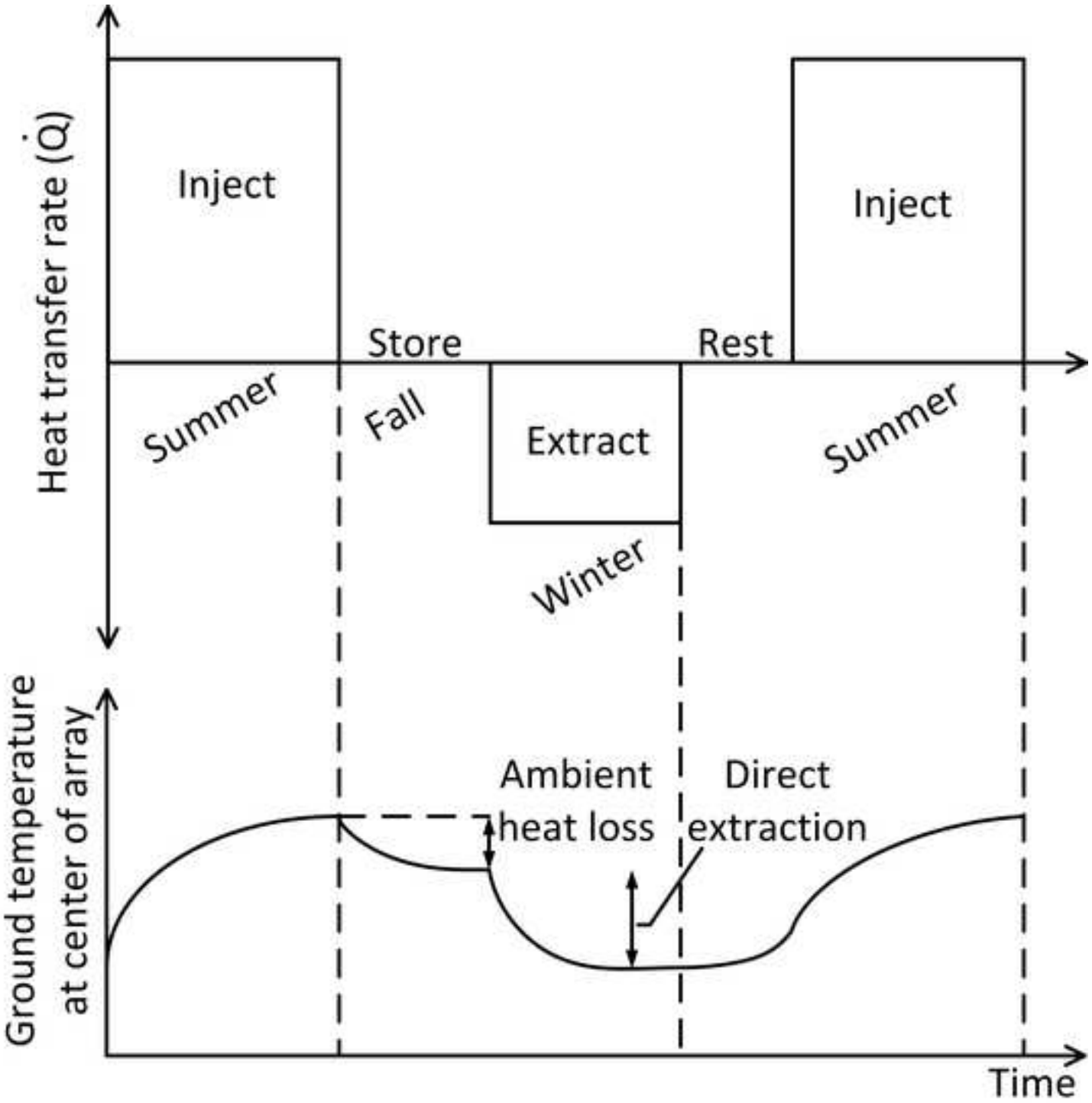

Figure 2
Click here to download Figure: Fig 2.tif

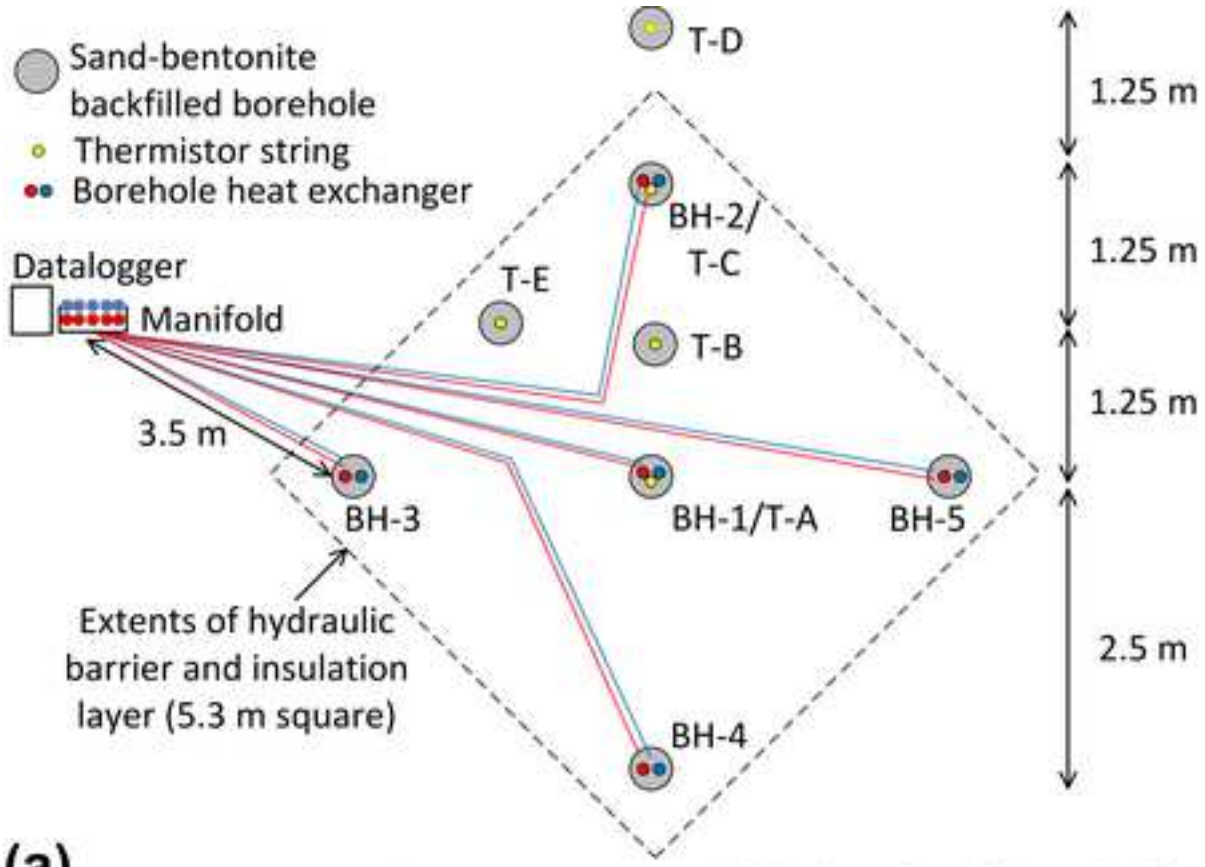

(a)

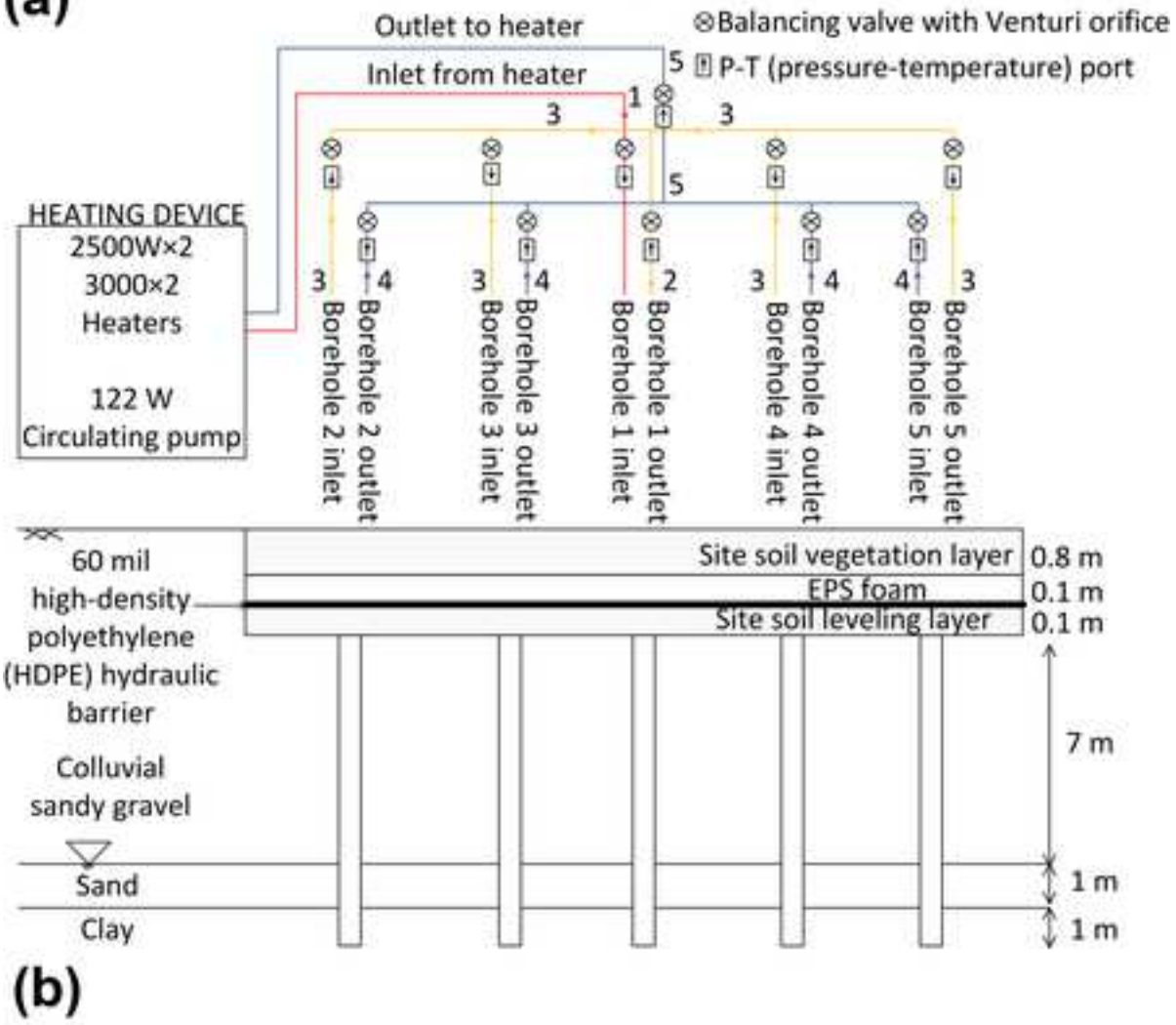

(b)

Figure 3
Click here to download Figure: Fig 3.tif

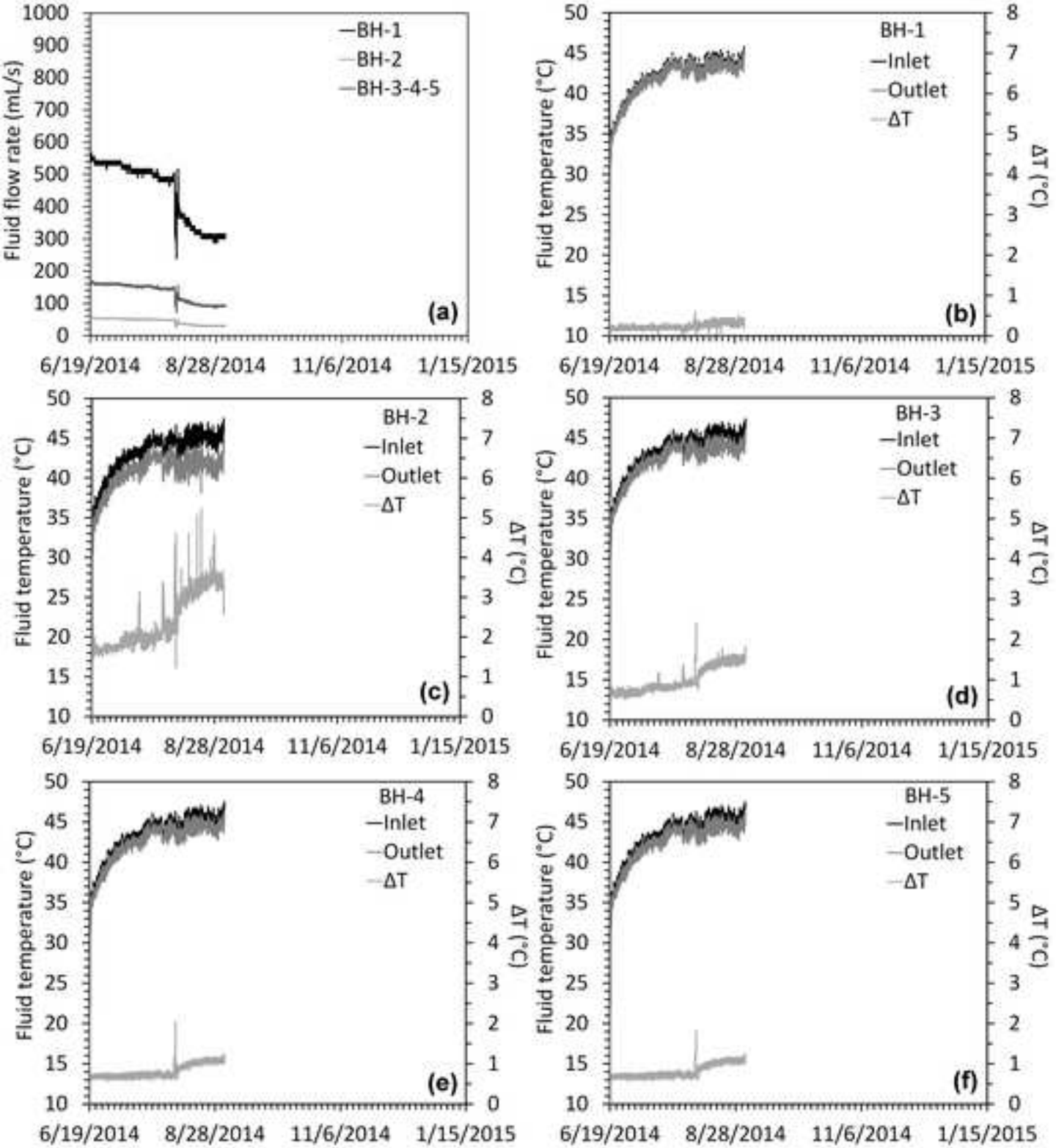

Figure 4
Click here to download Figure: Fig 4.tif

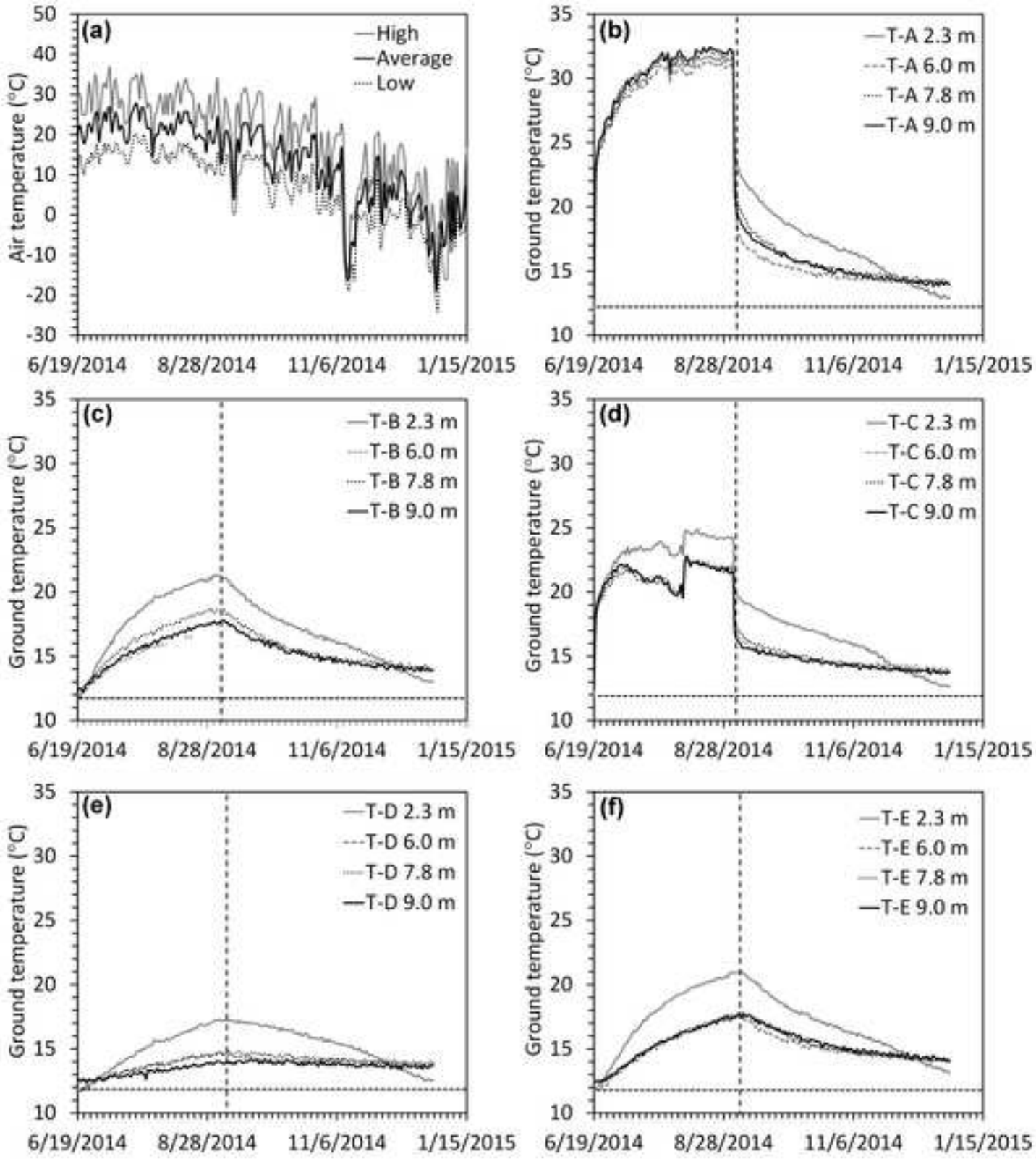

Figure 5
Click here to download Figure: Fig 5.tif

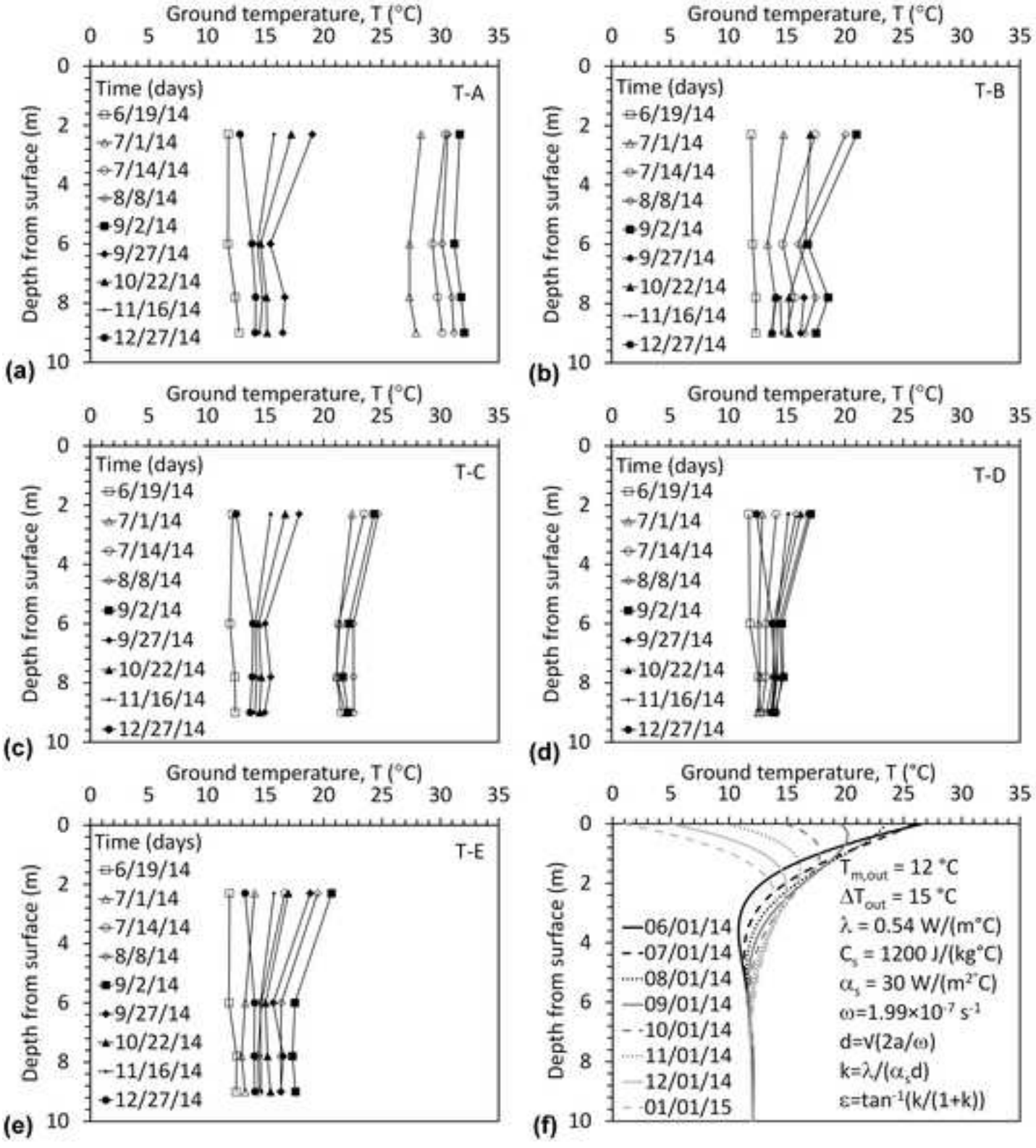

Figure 6
Click here to download Figure: Fig 6.tif

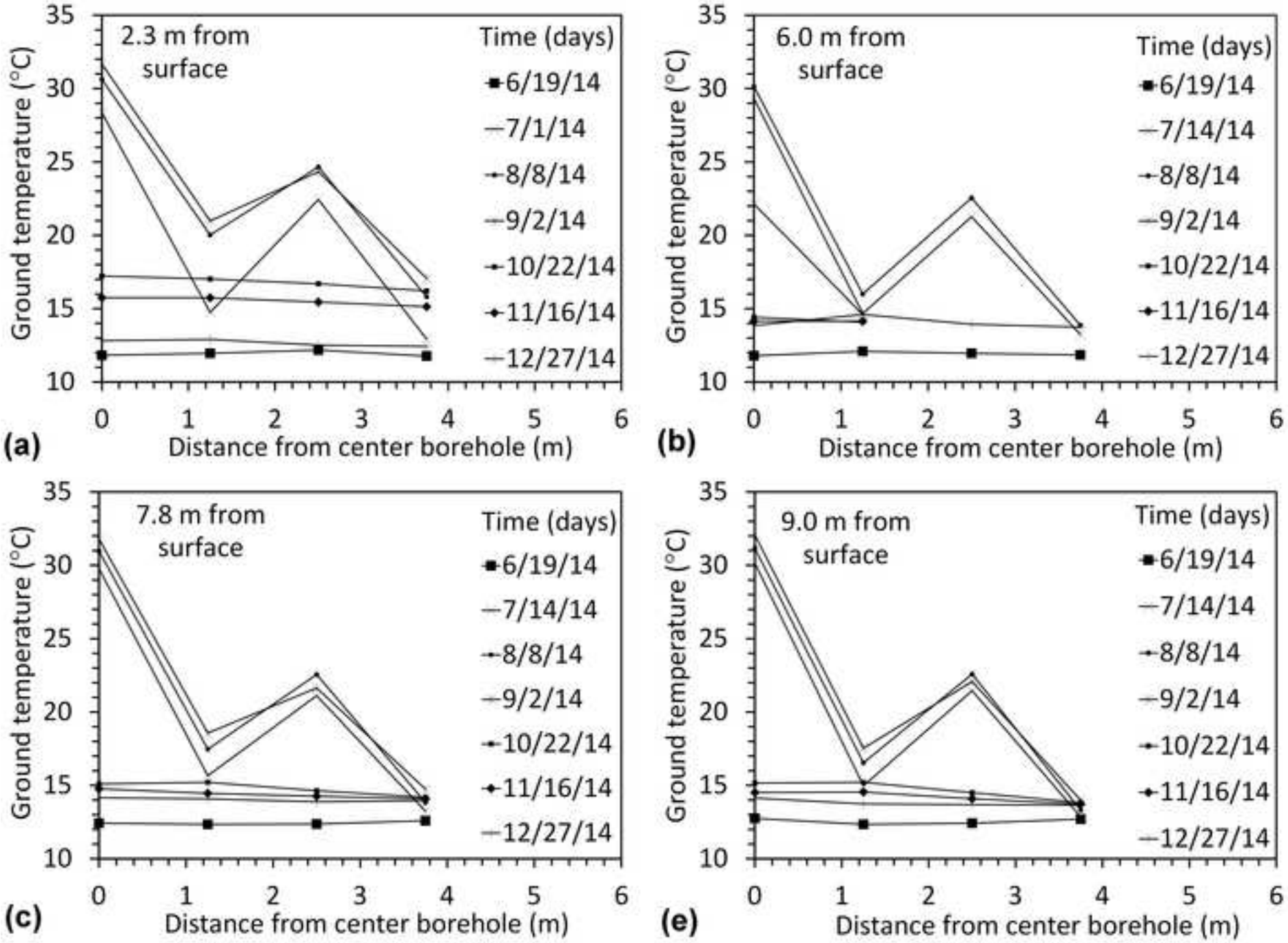

Figure 7
Click here to download Figure: Fig 7.tif

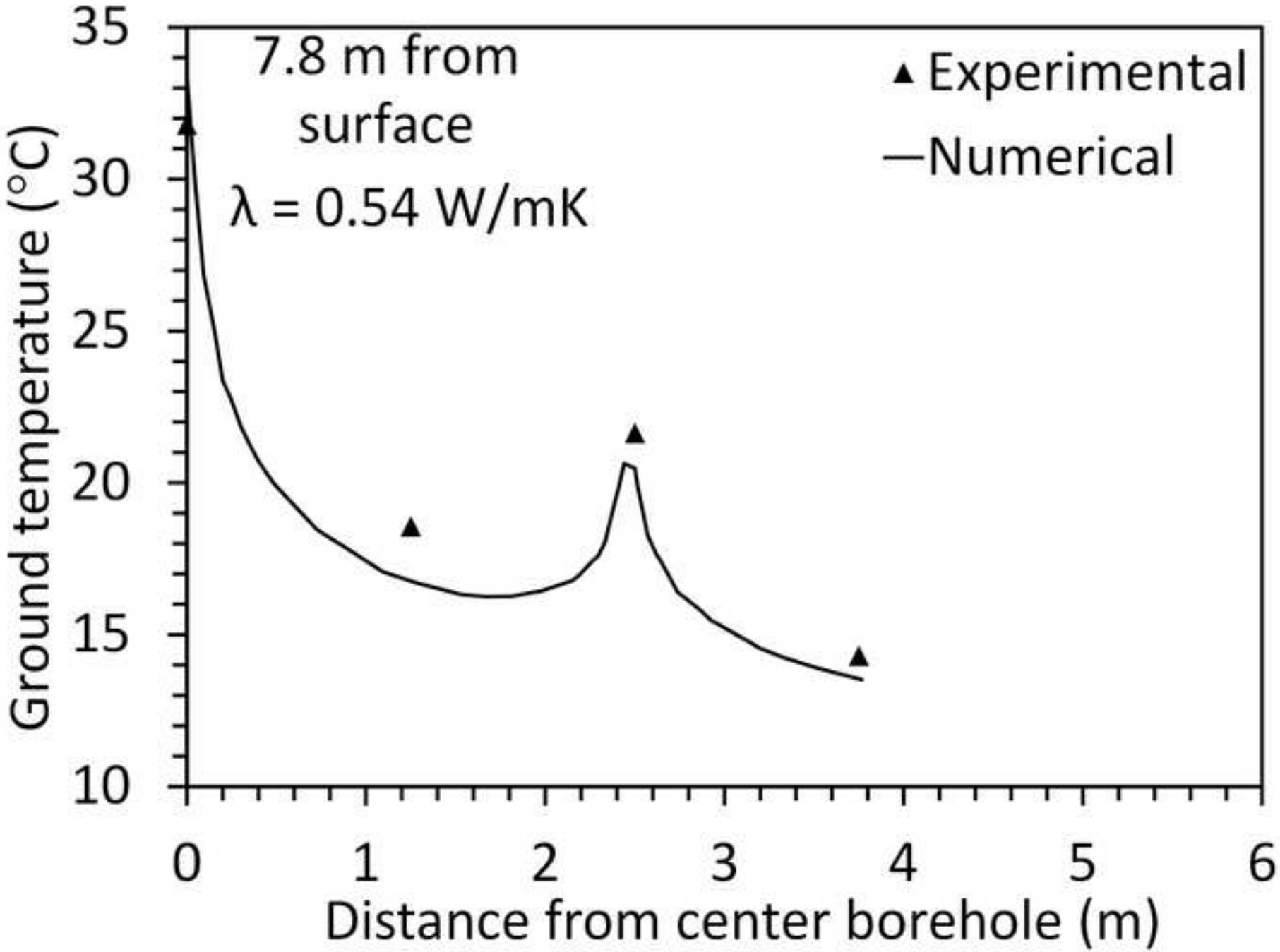

Figure 8
Click here to download Figure: Fig 8.tif

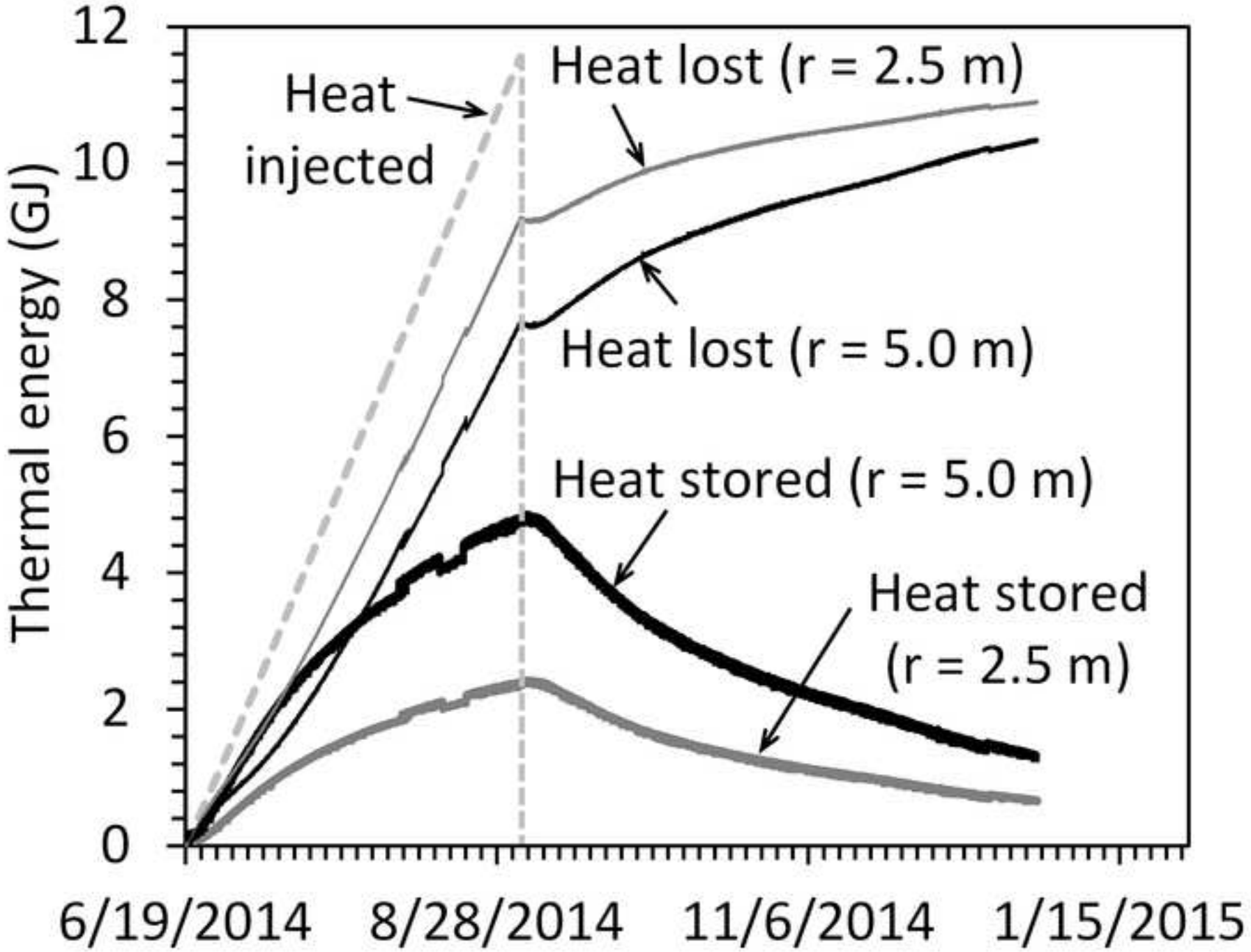

Figure 9
Click here to download Figure: Fig 9.tif